

**Manuscript version: Author's Accepted Manuscript**

The version presented in WRAP is the author's accepted manuscript and may differ from the published version or Version of Record.

**Persistent WRAP URL:**

<http://wrap.warwick.ac.uk/114693>

**How to cite:**

Please refer to published version for the most recent bibliographic citation information. If a published version is known of, the repository item page linked to above, will contain details on accessing it.

**Copyright and reuse:**

The Warwick Research Archive Portal (WRAP) makes this work by researchers of the University of Warwick available open access under the following conditions.

Copyright © and all moral rights to the version of the paper presented here belong to the individual author(s) and/or other copyright owners. To the extent reasonable and practicable the material made available in WRAP has been checked for eligibility before being made available.

Copies of full items can be used for personal research or study, educational, or not-for-profit purposes without prior permission or charge. Provided that the authors, title and full bibliographic details are credited, a hyperlink and/or URL is given for the original metadata page and the content is not changed in any way.

**Publisher's statement:**

Please refer to the repository item page, publisher's statement section, for further information.

For more information, please contact the WRAP Team at: [wrap@warwick.ac.uk](mailto:wrap@warwick.ac.uk).

**Full Paper**

**Covalent attachment of fibronectin onto emulsion-templated porous polymer scaffolds enhances human endometrial stromal cell adhesion, infiltration and function**

Sarah A. Richardson, Thomas M. Rawlings, Joanne Muter, Marc Walker, Jan J. Brosens,\* Neil R. Cameron\* and Ahmed M. Eissa\*

---

S. A. Richardson

Department of Chemistry, University of Warwick, Coventry, CV4 7AL, U.K.

T. M. Rawlings

Division of Biomedical Sciences, Reproductive Health Unit, Clinical Science Research Laboratories, Warwick Medical School, University of Warwick and Tommy's National Centre for Miscarriage Research, University Hospitals Coventry and Warwickshire NHS Trust, Coventry, CV2 2DX, U.K.

Dr. J. Muter

Division of Biomedical Sciences, Reproductive Health Unit, Clinical Science Research Laboratories, Warwick Medical School, University of Warwick and Tommy's National Centre for Miscarriage Research, University Hospitals Coventry and Warwickshire NHS Trust, Coventry, CV2 2DX, U.K.

Dr. M. Walker

Department of Physics, University of Warwick, CV4 7AL, U.K.

Prof. J. J. Brosens

Division of Biomedical Sciences, Reproductive Health Unit, Clinical Science Research Laboratories, Warwick Medical School, University of Warwick and Tommy's National Centre for Miscarriage Research, University Hospitals Coventry and Warwickshire NHS Trust, Coventry, CV2 2DX, U.K.

E-mail: J.J.Brosens@warwick.ac.uk

Prof. N. R. Cameron

Department of Materials Science and Engineering, Monash University, Clayton, 3800, Victoria, Australia.

School of Engineering, University of Warwick, Coventry, CV4 7AL, U.K.

E-mail: Neil.Cameron@monash.edu

Dr. A. M. Eissa

Department of Chemistry, University of Warwick, Coventry, CV4 7AL, U.K.

School of Engineering, University of Warwick, Coventry, CV4 7AL, U.K.

Department of Polymers, Chemical Industries Research Division, National Research Centre (NRC), El Bohouth St. 33, Dokki, Giza, 12622, Cairo, Egypt.

E-mail: A.M.Eissa@warwick.ac.uk

---

A novel strategy for the surface functionalisation of emulsion-templated highly porous (polyHIPE) materials as well as its application to in vitro 3D cell culture is presented. A heterobifunctional linker that consists of an amine-reactive N-hydroxysuccinimide (NHS) ester and a photoactivatable nitrophenyl azide, N-sulfosuccinimidyl-6-(4'-azido-2'-nitrophenylamino)hexanoate (sulfo-SANPAH), is utilized to functionalize polyHIPE surfaces. The ability to conjugate a range of compounds (6-aminofluorescein, heptafluorobutylamine, poly(ethylene glycol) bis-amine (PEG bis-amine) and fibronectin) to the polyHIPE surface is demonstrated using fluorescence imaging, FTIR spectroscopy and X-ray photoelectron spectroscopy (XPS). Compared to other existing surface functionalization methods for polyHIPE materials, this approach is facile, efficient, versatile and benign. It can also be used to attach biomolecules to polyHIPE surfaces including cell adhesion-promoting extracellular matrix (ECM) proteins. Cell culture experiments demonstrated that the fibronectin-conjugated polyHIPE scaffolds improved the adhesion and function of primary human endometrial stromal cells. It is believed that this approach can be employed to produce the next generation of polyHIPE scaffolds with tailored surface functionality, enhancing their application in 3D cell culture and tissue engineering whilst broadening the scope of applications to a wider range of cell types.

## 1. Introduction

It has been demonstrated that cells cultured in 3D exhibit a phenotype more akin to their counterparts *in vivo* than cells grown in 2D monolayer culture.<sup>[1-3]</sup> It is evident that 3D tissue culture models display enhanced cell-cell interactions, cell-ECM interactions and increased cell populations compared to 2D cultures.<sup>[4]</sup> To direct tissue formation in 3D, a scaffold is required to mimic the microenvironment for cells, providing mechanical support while directing cell adhesion, proliferation, differentiation, morphology and gene expression.<sup>[5,6]</sup> Highly porous polymers serve as efficient scaffolds for 3D cell culture. They can be prepared by emulsion templating methods whereby a high internal phase emulsion (HIPE) is created in which the continuous (non-droplet) phase contains polymerizable monomer(s) and the internal (droplet) phase occupies a total volume of 74% or greater, dispersed dropwise within the continuous phase. Polymerization then results in a well-defined macroporous polymer known as a polyHIPE. As a result of the removal of the internal droplet phase, polyHIPEs possess an interconnected network of pores of dimensions in the range of 10 – 100  $\mu\text{m}$ . Macroporous polymers with well-defined porosities and high specific surface areas are utilized in a wide range of applications including, but not limited to, media for gas storage,<sup>[7]</sup> catalysts,<sup>[8]</sup> enzyme supports<sup>[9]</sup> as well as scaffolds for tissue engineering<sup>[10,11]</sup> and *in-vitro* 3D cell culture.<sup>[12,13]</sup>

The majority of polyHIPE materials are synthesized by free radical polymerization initiated either thermally or photochemically; however, other methods have been reported.<sup>[14,15]</sup> PolyHIPE materials are versatile due to the ability to tune their chemical, physical and mechanical properties by careful choice of monomers.<sup>[16-19]</sup> These materials are attractive due to their high level of control over porosity and pore diameter,<sup>[20,21]</sup> which are essential characteristics when developing scaffolds for tissue engineering. However, these materials are typically constrained due to their lack of functionality; chemical functionalization is thus an attractive tool to enhance the functionality of polyHIPE surfaces. Surface functionalization can be achieved either by incorporating a functional comonomer<sup>[4]</sup> into the HIPE or *via* a post-

functionalization approach.<sup>[22,23]</sup> Recent work has explored the addition of the reactive comonomer pentafluorophenyl acrylate (PFPA) as a route to introducing functionality.<sup>[17]</sup> Amidation of the penta-fluorophenyl ester allowed functional amine-bearing molecules to be added to the polyHIPE surface; however, emulsion destabilization occurred when over 50 wt% of PFPA was added, leading to phase separation. Post-polymerization allows for greater control over the porous structure and is the most attractive method to enhance functionality whilst not deteriorating the morphology or the possibility of affecting emulsion stability. A desired pore diameter dictated by the internal phase can be obtained, then functionality added. Several routes to post-polymerization have been explored.<sup>[24]</sup> Residual unreacted thiols have been exploited as reactive handles to functionalize thiol-acrylate polyHIPEs. Post-polymerization functionalization of these has been explored by both thermal- and UV-initiated radical reactions and amine-catalyzed Michael addition reaction.<sup>[23]</sup> Glycidyl methacrylate<sup>[19]</sup> and acrylate esters such as N-acryloxysuccinimide<sup>[9]</sup> have been used as co-monomers in polyHIPE formulations, allowing for post-polymerization functionalization. Poly(4-vinylbenzyl chloride-co-divinylbenzene) polyHIPE materials were functionalized with a range of nucleophiles with high degrees of conversion, leading to monolithic supports and scavengers.<sup>[20]</sup> Surface functionalization using dithiophenol maleimide as a linker to conjugate responsive functional macromolecules has also been investigated. Functionalization was observed to be reversible upon addition of thiol-containing glutathione, resulting in switchable surface properties.<sup>[25]</sup>

N-sulfosuccinimidyl-6-(4'-azido-2'-nitrophenylamino)hexanoate (sulfo-SANPAH) is a bifunctional photolinker that contains two functional groups (azido group and NHS ester group). Sulfo-SANPAH has previously been used to conjugate biomolecules to polymeric surfaces, such as poly(dimethylsiloxane), and to hydrogels, to promote cell adhesion and function. The conjugation procedure is versatile, efficient and can be accomplished in two reaction steps under aqueous conditions, making this approach an excellent alternative method for surface functionalisation with biomolecules. Reported applications of sulfo-SANPAH-

modified biomaterial surfaces include enhancing adhesion, proliferation, migration and differentiation of pre-osteoblastic MC3T3-E1 cells on the surface of type I collagen–modified hydrogels.<sup>[26]</sup> ~~The combination of polyacrylamide (PA) hydrogels and varying concentrations of sulfo-SANPAH was explored to investigate substrate stiffness, porosity and ligand tethering. Treating PA hydrogels with increasing concentrations of sulfo-SANPAH increased fibrous collagen tethering and decreased the deflection of the collagen fiber segment at rupture.<sup>[27]</sup>~~ Attaching biomolecules (such as fibronectin) to increase functionality can provide an improved microenvironment for several types of regenerative cells.<sup>[27,28]</sup> Herein, we demonstrate that sulfo-SANPAH can be used to conjugate fibronectin (as a model ECM protein) to polyHIPE scaffolds resulting in enhanced adhesion, infiltration and function of cultured primary human endometrial cells.

## **2. Experimental Section**

### **2.1. Materials**

The monomers trimethylolpropane triacrylate (TMPTA) and trimethylolpropane tris (3-mercaptopropionate) (TMPTMP) were obtained from Sigma Aldrich. The photoinitiator, diphenyl (2,4,6- trimethyl benzoyl)–phosphine oxide/ 2-hydroxy-2-methylpropiophenone and solvent 1,2-dichloroethane were obtained from Sigma Aldrich. The surfactant, Hypermer B246 (a block copolymer of polyhydroxystearic acid and polyethylene glycol) was obtained from Croda. All materials were used as supplied without any further purification. Sulfo-SANPAH and dimethyl sulfoxide (DMSO) were obtained from Thermo Fischer Scientific without further purification. 6-aminofluorescein, fibronectin, heptafluorobutylamine and poly(ethylene glycol) bis-amine (PEG-bis) were obtained from Sigma Aldrich and used without further purification.

All materials used for the isolation, tissue digestion and culturing of primary endometrial cells have been published by Barros et al.<sup>[29]</sup> Phenol-free DMEM/F12 media with HEPES and L-Glutamine, fetal bovine serum, and 100×Antibiotic-Antimycotic solution were purchased from Thermo Fisher Scientific. 8-Bromo-cyclic adenosine monophosphate (cAMP) and medroxyprogesterone 17-acetate (MPA) were obtained from Sigma Aldrich. Nuclease-free water was obtained from Ambion. QunatiTect Reverse Transcription Kit was obtained from QIAGEN. Chloroform, isopropanol and ethanol were obtained from Sigma Aldrich. Tris-EDTA buffer was obtained from Sigma Aldrich. SyBr Green was obtained

from Applied Biosystems. Forward and reverse PCR primers for *PRL* and *L19* were obtained from Peptidech.

## **2.2. Methods**

### **2.2.1. PolyHIPE Synthesis**

The oil phase, consisting of TMPTMP, TMPTA, 1,2-dichloroethane, Hypermer B246 and diphenyl (2,4,6-trimethylbenzoyl) phosphine oxide/2-hydroxy-2-methyl-propiophenone blend was added to a 3-necked 250 mL bottom flask with continuous stirring at 350 rpm from a paddle stirrer. To form the HIPE, 56 mL of water was added dropwise to the solution down dropping funnel positioned in one of the necks in the flask. Once all the water has been added, allow for further stirring to allow the emulsion to become homogenous. A 1.1 molar ratio of thiol and acrylate was used and the emulsion aqueous phase content was 80% (v/v). The emulsion was poured into a PTFE mould (diameter 15 mm, depth 30 mm) and secured between two glass plates and irradiated using a Fusion UV Systems Inc. Light Hammer® 6 variable power UV curing system with LC6E benchtop conveyor. The system was fitted with a H – bulb, UV radiation is emitted between 200-450 nm and the maximum intensity is 200 W cm<sup>-2</sup>. The material was irradiated six times on either side of the PTFE mould at a belt speed of 5.0 m/min, to ensure complete curing. The cured polyHIPEs were washed by immersing in acetone for 1 hour, then dried. Further washing was carried out by Soxhlet extraction with DCM overnight. The PolyHIPE was then left to dry under high vacuum for several hours. The material was sliced using a microtome into discs of 200 mm thick and 10 mm diameter.

### **2.2.2. Sulfo-SANPAH Functionalization**

PolyHIPE scaffolds were first hydrated gradually by immersion in 100% ethanol followed by 70% ethanol to render the scaffolds more hydrophilic. After removal of ethanol, a 1 mL of sulfo-SANPAH aqueous solution (0.5 mg/mL or 2.0 mg/mL) was added to a glass vial containing a polyHIPE scaffold 200 mm thick and 10 mm diameter (ca. 5 mg). The scaffolds were then irradiated 6 times with the UV Light Hammer system used in polyHIPE preparation (as described above) to allow sulfo-SANPAH to conjugate to the scaffold. The sulfo-SANPAH solution was removed by filtration and the scaffolds were washed twice with deionized water and then lastly once with ethanol to remove any unreacted residues. The scaffolds were then left to air-dry for several hours.

### **2.2.3. Post-functionalization**

6-aminofluorescein, heptafluorobutylamine and PEG-bis (0.05 wt% or 0.20 wt% relative to a 1:1 molar ratio of their molecular weights) were dissolved in 0.5 mL of tetrahydrofuran (THF). 100 µL of fibronectin solution was diluted in 200 µL of PBS. Scaffolds were left in their chosen solvent for 72

hours. The solution was removed and the scaffolds were washed three times in their chosen solvent to remove any residues. The scaffolds were then left to air-dry for several hours.

#### **2.2.4. Endometrial Biopsy and Isolation of Endometrial Stromal Cells**

Endometrial biopsies were obtained from patients attending the Implantation Clinic, a dedicated research clinic at University Hospitals Coventry and Warwickshire (UHCW) NHS Trust, Coventry, U.K. All research was undertaken with NHS National Research Ethics Committee approval (1997/5065). All biopsies were retrieved from the Arden Tissue Bank at UHCW. All participants provided written informed consent in accordance with the guidelines of the Declaration of Helsinki, 2000. Tissue digestion and isolation of human endometrial stromal cells procedures are referred to in the published protocol by Barros et al.<sup>[29]</sup> Primary endometrial stromal cells were isolated from 3 different biopsies. Primary cells then pooled and all cell culture experiments performed in triplicate.

#### **2.2.5. Culturing of Cells**

Primary human endometrial stromal cells were cultured DMEM/F-12 containing 10% dextran-coated charcoal-treated fetal bovine serum (DCC-FBS), L-glutamine (1%) and 1% antibiotic-antimycotic solution until ~90% confluency before being passaged twice into T75 flasks. The culture media and 0.25% trypsin-EDTA were pre-heated in the water bath to 37 °C. The media was aspirated and 10 mL of PBS was added, rinsed around the flask and then aspirated. 1 mL of 0.25% trypsin-EDTA was added making sure it covered the cells and placed in the incubator for 5 minutes until the cells had dislodged, which was checked under the microscope. Gentle agitation of the flasks was used to loosen the cells from the flask. Culture media (9 ml) was added into the flask to neutralise the trypsin, the media was pipetted repeatedly so the cells were collected from the bottom of the flask. The solution was transferred into 15 mL Falcon tubes and centrifuged for 5 minutes (at 1200 rpm at 280 × g) at room temperature. The media was aspirated leaving the pellets of cells behind. The pellets were re-suspended in 9 mL of culture media and placed back into a new T75 flask. This was repeated twice. After expansion of two passages, the cells were detached for the cell-seeding experiments. A cell counter (LUNA™ automated cell counter ) was used to determine cell number prior to seeding.

#### **2.2.6. Seeding Cells onto 3D Scaffolds**

Scaffolds were placed into 24 well plates, the scaffolds without functionalised compounds were disinfected with 100% ethanol and then rendered hydrophilic with 70% ethanol, twice. All scaffolds are washed twice with phosphate buffered saline (PBS). The discs were left in PBS before the cells were seeded. Fibronectin solution (300 µL; 0.33 mg/mL in PBS) was added to each scaffold. Scaffolds coated with fibronectin were left for 1 hour to stand at room temperature. Inserts to hold down the scaffolds were washed thoroughly in ethanol for sterilisation and then rinsed twice in PBS. Before seeding cells, all excess fluid was aspirated from the wells. Cells were seeded on the top of the scaffold at a density of

(Experiment 1:  $1.9 \times 10^5$ , Experiment 2:  $2.2 \times 10^5$  and Experiment 3:  $2.6 \times 10^5$ .) The cells were then allowed to settle onto the scaffold for 60-90 minutes. Inserts were then placed on top of each scaffold before carefully adding 2000  $\mu$ L of culture media into each well. Media was changed every other day for up to 9 days and fixated at Day 2, Day 5 and Day 9.

### **2.2.7. Fixating cells onto 3D Scaffolds**

Media was aspirated from the wells and the scaffolds were washed in 2 mL of sterile PBS. The scaffolds were transferred to vials containing 4% formaldehyde and stored at 4 °C prior to H&E Staining.

### **2.2.8. Decidualisation of HESCs**

Cells were down-regulated for several hours in phenol red-free DMEM/F12 containing 2% DCC-FBS and then subjected to a reverse decidualization time-course. The scaffolds and parallel 2D cultures were decidualized with 0.5 mM cAMP) and  $10^{-6}$  M medroxyprogesterone acetate (MPA) in phenol red-free DMEM/F12 containing 2% DCC-FBS for 8 days (see **Table SI-1**). Decidualization medium was changed every other day.

### **2.2.9. RNA Isolation from Cells in Scaffolds**

Cells were washed with PBS and harvested after the addition of phenol-guanidinium thiocyanate monophasic solution (STAT-60). The homogenate was transferred into an RNase-free tube, add 80 mL of chloroform was added and the tube was agitated to form a homogenous mix for 15 seconds. Tubes were centrifuged at 16000 g for 15 min at 4 °C to separate the three phases, upper phase where the RNA remains, from the white interphase and lower red phenol chloroform phase where the DNA and protein is found. The aqueous phase was transferred to a fresh tube containing half of the original STAT – 60 volume of isopropanol and 20 mL of glycogen. Tubes were vortexed and stored at -80 °C for 30 minutes. Tubes were centrifuged at 12000 g for 10 minutes at 4 °C where RNA precipitate was formed. RNA pellets were washed twice in 75 % ethanol in nuclease free water and the pellet was air-dried for 2 minutes before resuspension in Tris-EDTA buffer and purity was measured using a Nanodrop spectrophotometer.

### **2.2.10. cDNA synthesis from RNA**

QuantiTect Reverse Transcription Kit (QIAGEN) was used for cDNA synthesis. The volume of RNA was calculated depending on the amount of RNA that was quantified. The RNA, 2 mL of gDNA buffer and nuclease free water were added to total 12 mL IN Eppendorf tubes. Tubes were briefly vortexed and incubated at 42 °C for 2 minutes. The reverse transcription master mix required: 4  $\mu$ l RT Buffer (5 $\times$ ), 1  $\mu$ l RT Primer Mix and 1 $\mu$ l Quantiscript Reverse Transcriptase and was then vortexed. A control sample

of the reverse transcriptase was prepared without the enzyme. Tubes were then incubated at 42 °C for 30 minutes then incubated at 95 °C for 3 minutes. Samples were stored at -20 °C.

### **2.2.11. Real Time Quantitative Polymerase Chain Reaction (RTq-PCR)**

A real-time PCR instrument (7500 Real-Time PCR system, Applied Biosystems) was used for amplification and quantification of *PRL* gene expression. Briefly, 0.3 mL of forward and reverse primers, 10 mL of SYBR Green and 8.4 mL of nuclease-free water was formed to make a master mix to distribute in a 96 well plate. The same was carried out for *L19* expression, encoding the house keeping gene ribosomal protein L19. Total RNA ( $x \mu\text{g}$ ) suspended in 1 ml was then added to each well. Plates were centrifuged at 1100 g for 3 minutes. The housekeeping gene, *L19*, was used to normalise the data between the samples. Controls were used by replacing the RNA with nuclease free water. A threshold was assigned with a peak to define a cycle threshold (Ct) value.

## **2.3. Characterization**

### **2.3.1. FTIR Spectroscopy**

All FTIR – ATR spectra were obtained using a Bruker Vector 22 using Opus software at wavenumbers between  $0 \text{ cm}^{-1} - 4000 \text{ cm}^{-1}$

### **2.3.2. Scanning Electron Microscopy**

PolyHIPE morphology was investigated using a ZEISS SIGMA SEM. Fractured polyHIPE pieces were sputter-coated with gold using a Cressington sputter coating system and mounted on carbon fibre pads adhered to aluminium stubs. Average void diameters were then calculated using Image J Version 1.50i. One hundred voids were randomly chosen from an SEM image of the sample and the diameters measured. Void diameters measured using this method underestimate the true value as the voids are unlikely to be exactly bisected. Therefore a statistical correction factor was used to account for this underestimate.<sup>[30]</sup>

### **2.3.3. X-ray photoelectron Spectroscopy**

X-Ray photoelectron spectroscopy (XPS) analysis was performed using a Kratos Axis Ultra DLD spectrometer at the University of Warwick. The scaffolds were cut to suitable size and attached to double sided carbon tape and mounted onto a stainless steel bar. The surface composition of the modified scaffolds was characterized. The data was subsequently charge corrected using the C-C/C-H peak at 284.6 eV as a reference. The measurements were conducted at room temperature and at a take-off angle of 90° with respect to the surface. Survey spectra were acquired to determine the elemental composition of the surface. High-resolution spectra of the principle core level of each element present were then acquired for chemical state identification. Both survey and core level XPS spectra were recorded from

a surface area of  $300 \times 700 \mu\text{m}$ , with such a large area, it is deemed to be representative of the whole sample surface. Data were analysed using the Casa XPS software, using Gaussian – Lorentzian (Voigt) line shapes and Shirley backgrounds.

#### **2.3.4. Haematoxylin – Eosin (H&E) Staining**

Formaldehyde-fixed discs were processed and embedded in paraffin and 5 mm sections were obtained with a microtome. Sections were mounted onto glass slides and placed in an incubator overnight at 60 °C. Slides were rehydrated in xylene for 5 minutes followed by 100% isopropanol for 2 minutes. Then the slides were dipped in 70% isopropanol for 2 minutes then washed in distilled water for another 2 minutes. Haematoxylin was added to the slides for 1 minute then rinsed with distilled water for 15 minutes. Then the cells were stained with eosin-Y for 1 minute. Finally, the slides were immersed in 95% ethanol then 100% ethanol then xylene for 2 minutes each. The slides were then mounted with coverslips using distyrene/plasticizer/xylene (DPX).

#### **2.3.5. Cell Imaging**

Invitrogen EVOS FL Cell Imaging System was used to image stromal cells and histology slides.

### **3. Results and Discussion**

The parent material that we have chosen to functionalize is a thiol-acrylate polyHIPE that has been previously reported.<sup>[18]</sup> Trimethylolpropane tris (3-mercaptopropionate) (TMPTMP) and trimethylolpropane triacrylate (TMPTA) were utilized to prepare a HIPE that was subsequently photopolymerized, producing polyHIPE materials of 80 % porosity and with a well-defined morphology, determined by the aqueous internal phase. The characteristic interconnected open cell morphology of the polyHIPEs was characterized using scanning electron microscopy (SEM) and the average pore diameter calculated by image analysis was found to be between 20 and 30  $\mu\text{m}$ , as displayed in **Figure 1**. Reproducibility of different batches of polyHIPEs morphology can be found in the ESI Figure SI-1.

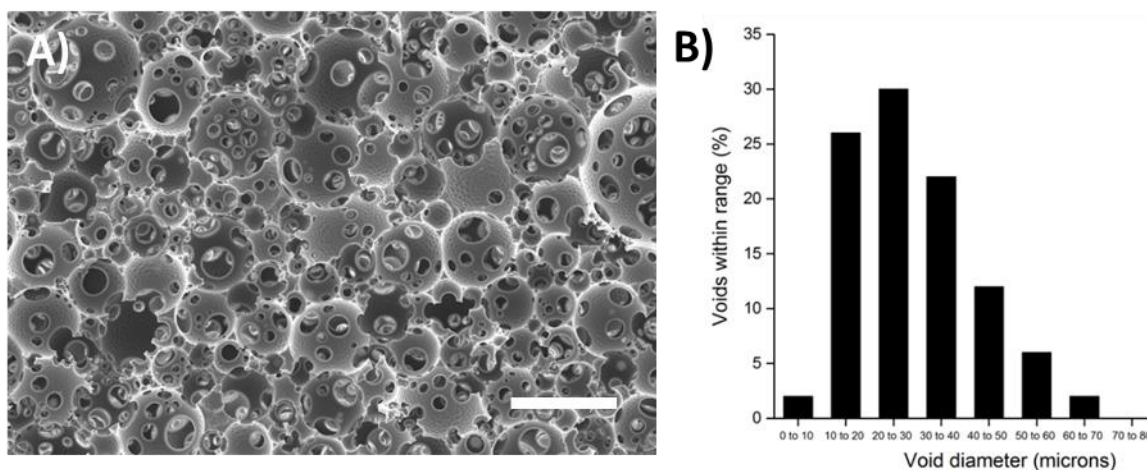


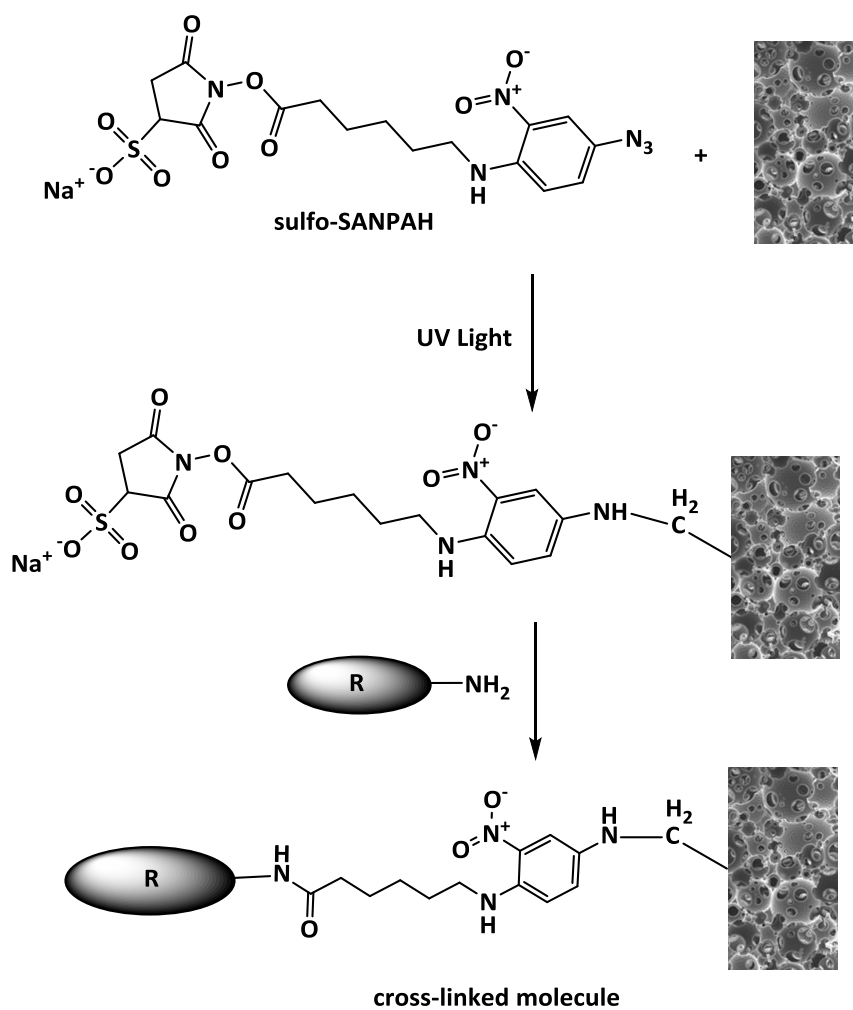
**Figure 1.** A) SEM showing the morphology of the polyHIPE material. Scale bar = 50  $\mu\text{m}$  and B) the void diameter distribution determined by analysis of SEM images.

The polyHIPE surfaces were treated with low (0.05 wt %) and high (0.20 wt %; relative to the total weight of the polyHIPE monoliths) concentrations of aqueous solutions of sulfo-SANPAH, a heterobifunctional compound that consists of an amine reactive N-hydroxysuccinimide (NHS) ester and a photoactivatable nitrophenyl azide (**Scheme 1**). When exposed to UV light, the nitrophenyl azide forms a nitrene group that can insert into C-H bonds on the polyHIPE material, leading to a homogenous distribution of sulfo-SANPAH groups on the surface. Sulfo-SANPAH is supplied as a sodium salt, it is useful for cell-surface protein crosslinking and possesses charged groups for water solubility to a concentration of 10 mM. It was found that, upon reactions with different concentrations of sulfo-SANPAH solutions, the polyHIPE materials undergo a colour transition from white to various shades of pink, providing a simple visual confirmation of the successful photo-reaction, as shown in Figure 2. There was no visible influence of surface functionalization on the morphology, as shown in the ESI Figure SI-2.



**Figure 2.** Photographs of polyHIPEs (left to right) unfunctionalized, sulfo-SANPAH at 0.05 wt % concentration, sulfo-SANPAH at 0.20 wt % concentration.

The NHS ester group of the sulfo-SANPAH can be subsequently reacted with primary amine-containing compounds to form stable amide bonds, resulting in the release of sulfo-NHS. Sulfo-SANPAH has a long spacer arm (18.2Å) which provides sufficient space between conjugated molecules and the desired surface.<sup>[31]</sup> Creating distance between the molecules and the polyHIPE scaffold can provide enhanced access required for integrin binding.<sup>[32,33]</sup> A number of amine-containing model compounds (6-aminofluorescein, poly(ethylene glycol) bis-amine (PEG-bis), 2,2,3,3,4,4,4-heptafluorobutylamine and fibronectin) were employed to investigate the efficiency and versatility of this photochemical approach as a route to the surface functionalization of polyHIPE materials (**Scheme 1**).



**Scheme 1.** Sulfo-SANPAH scheme displaying the two step conjugation to polyHIPE scaffold and R group. R = 6-aminofluorescein, heptafluorobutylamine, PEG-bis and fibronectin.

Following conjugation and extensive washing of the functional polyHIPE materials, 6-aminofluorescein-functionalized scaffolds became fluorescent under UV light, as shown in Figure 3.



**Figure 3.** Photographs (left to right) of unfunctionalized and sulfo-SANPAH-functionalized polyHIPE scaffolds reacted with heptafluorobutylamine (illuminated under UV light;  $\lambda = 254$

nm). Sulfo-SANPAH concentrations used were 0.05 wt% and 0.20 wt% (middle and right, respectively).

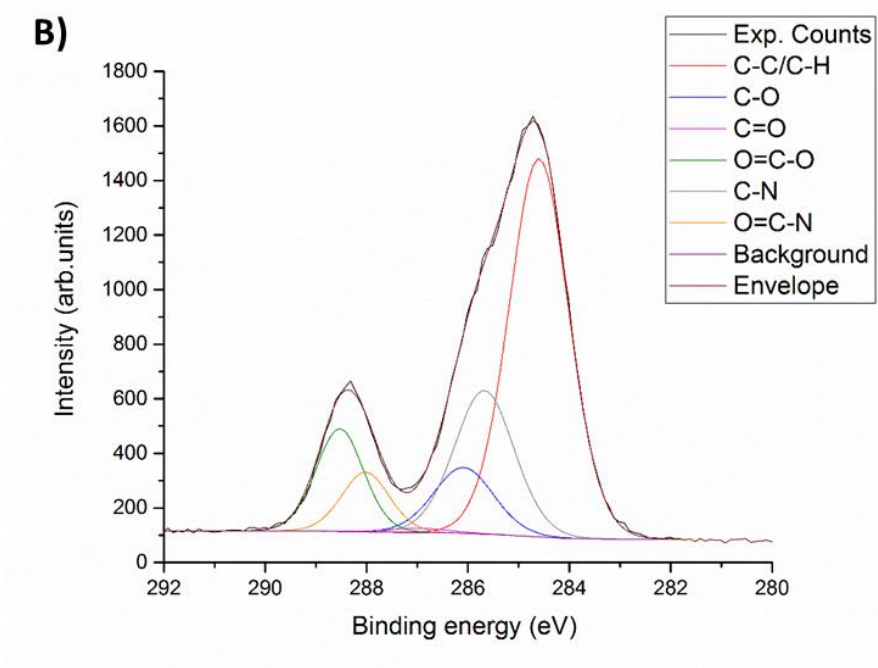
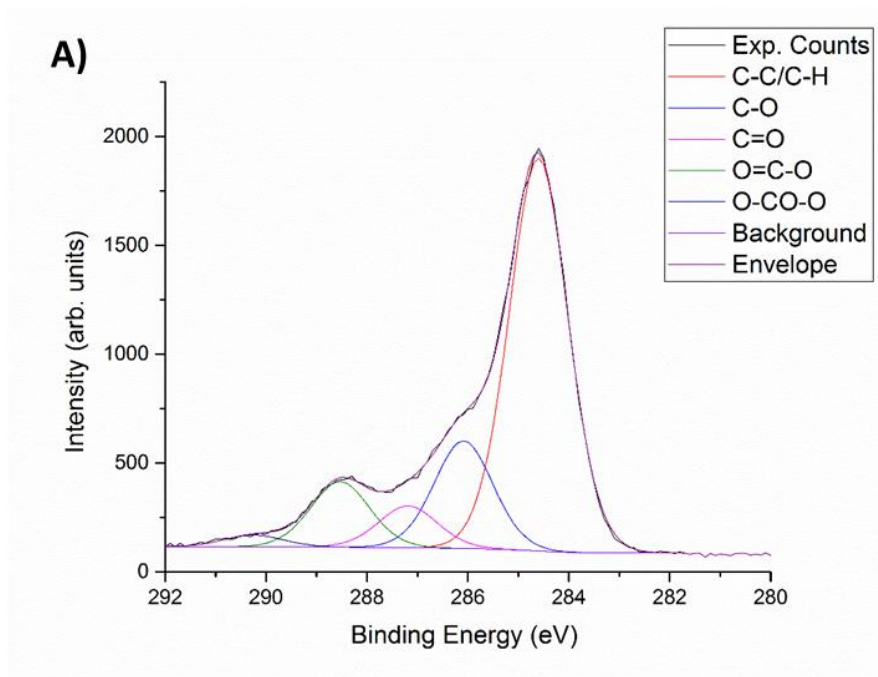
The functionalized scaffolds were analysed by X-ray photoelectron spectroscopy (XPS) to determine the atomic surface composition (**Table 1**). Composition profiles showing peak assignment and percentage of each C 1s component for unfunctionalized and functionalized polyHIPE materials are displayed in Table SI-2 in the ESI.

**Table 1.** Atomic compositions from XPS data of unfunctionalized and functionalized polyHIPE materials. Atomic percentages are accurate to +/- 2%.

Sample	Overall Composition (Atomic %)				
	C 1s	O 1s	S 2p	N 1s	F 1s
Unfunctionalized thiol – acrylate polyHIPE	80.65	17.44	1.61	0.00	0.00
Sulfo-SANPAH functionalized polyHIPE	69.25	25.07	4.10	1.18	0.00
Sulfo-SANPAH functionalized polyHIPE treated with 2,2,3,3,4,4,4 – heptafluorobutylamine	66.86	25.81	4.67	1.19	1.47
Sulfo-SANPAH functionalized polyHIPE treated with 6-aminoflourescein	67.02	27.13	4.43	1.42	0.00
Sulfo-SANPAH functionalized polyHIPE treated with bis amino PEG-bis	67.92	26.25	3.03	2.80	0.00
Sulfo-SANPAH functionalized polyHIPE treated with fibronectin	77.30	29.42	3.51	4.42	0.00

In order to identify the functional groups at the surface, the C 1s peak was modelled using the minimum number of synthetic components required to fit the raw data as shown in **Figure 4A**.

The unfunctionalized scaffold spectra displays five regions: C-C and C-H bonds (284.6 eV), C-O bonds (286.1 eV), C=O bonds (287.2 eV), O=C-O bonds (288.5 eV) and O-CO-O bonds (290.2 eV). This spectrum was then used as a reference for subsequent samples.



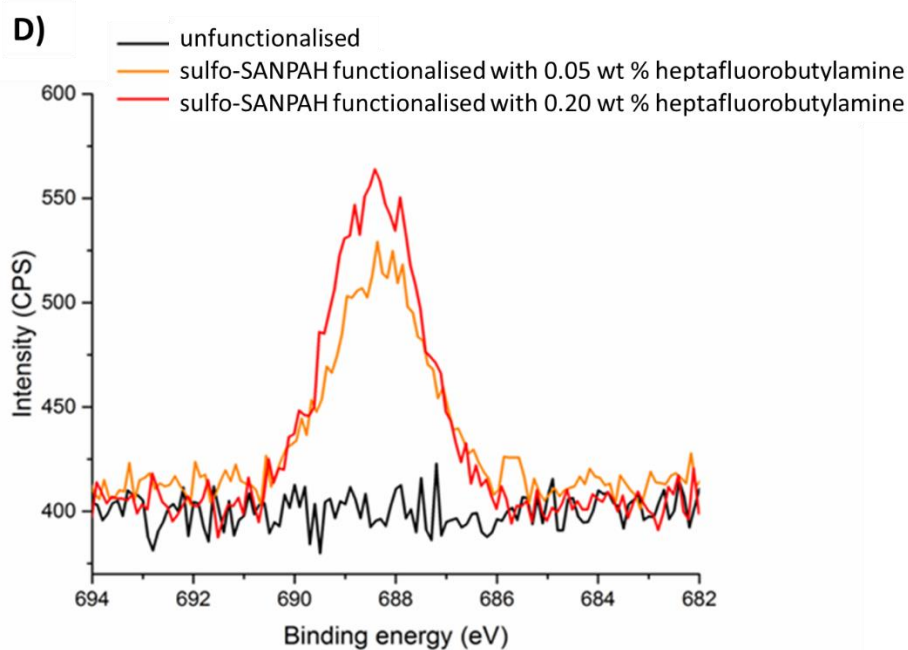
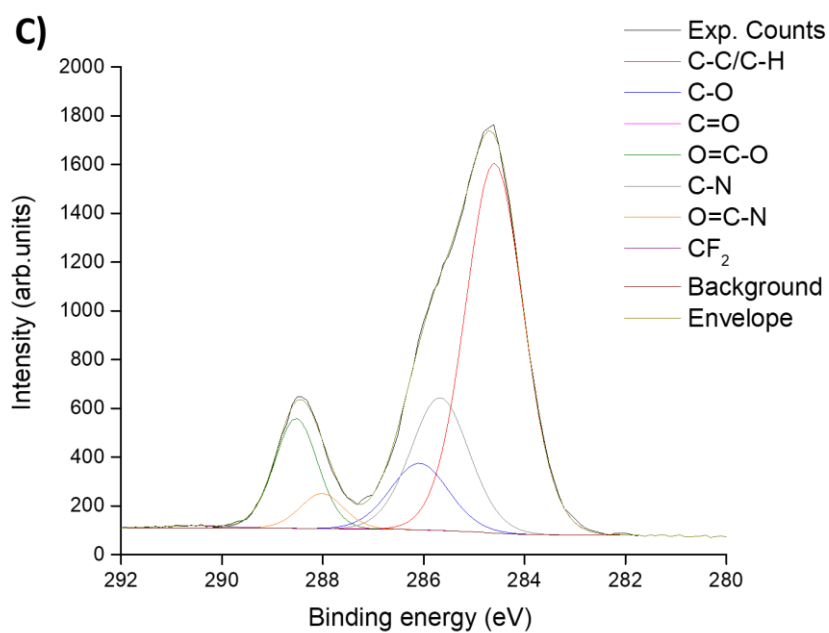


**Figure 4.** XPS high resolution peak-fitted C 1s spectra for A) unfunctionalized, B) sulfo-SANPAH and C) sulfo-SANPAH functionalized with heptafluorobutylamine. The binding environments of interest are denoted in the figure. D) high resolution F1s spectra for unfunctionalized and sulfo-SANPAH functionalized with heptafluorobutylamine at two different concentrations.

As expected, the unfunctionalized scaffold exhibits no contribution from C-N bonding. Upon functionalization with sulfo-SANPAH, nitrogen appears on the surface as demonstrated by the O=C-N bonding environment at 288.0 eV and the C-N bonding environment at 285.6 eV (**Figure 4B**). All other C 1s spectra can be found in ESI Figure SI-3. In addition, in the high resolution spectra, the N 1s peak at 399.4 eV displays an increase in nitrogen when functionalized with increasing concentrations of sulfo-SANPAH (Figure SI-4).

Overall, the composition of carbon decreases and oxygen increases when sulfo-SANPAH is conjugated to the polyHIPE surface, which is evident from **Table 1**. The bonding environments O=C-N and O=C-O decreased when compounds were conjugated *via* the NHS ester as shown in **Figure 4C** with sulfo-SANPAH treated with heptafluorobutylamine, when compared to **Figure 4B**. The spectra collected for the S 2p regions remain constant as there are no additional sulphur functional groups before or after conjugation. Heptafluorobutylamine was chosen due to its high fluorine content. The introduction of fluorine on the surface is shown by the CF<sub>2</sub> bonding environment at 290.5 eV in Figure 4C. The high resolution F 1s spectra shown in Figure 4D suggests that the higher the concentration of heptafluorobutylamine, the higher the fluorine content, with emissions from the F 1s energy level observed at 688.4 eV. FT-IR spectroscopy was used to show the presence of fluorine on the surface of the PolyHIPE materials (**Figure 5**). Contributions from F were observed at 948 cm<sup>-1</sup>, 1016 cm<sup>-1</sup> and 1409 cm<sup>-1</sup>. Amines were also observed as shown by N-H stretch at 3405 cm<sup>-1</sup> and C-N stretch at 1640 cm<sup>-1</sup> from sulfo-SANPAH conjugation and from the primary amine of heptafluorobutylamine.

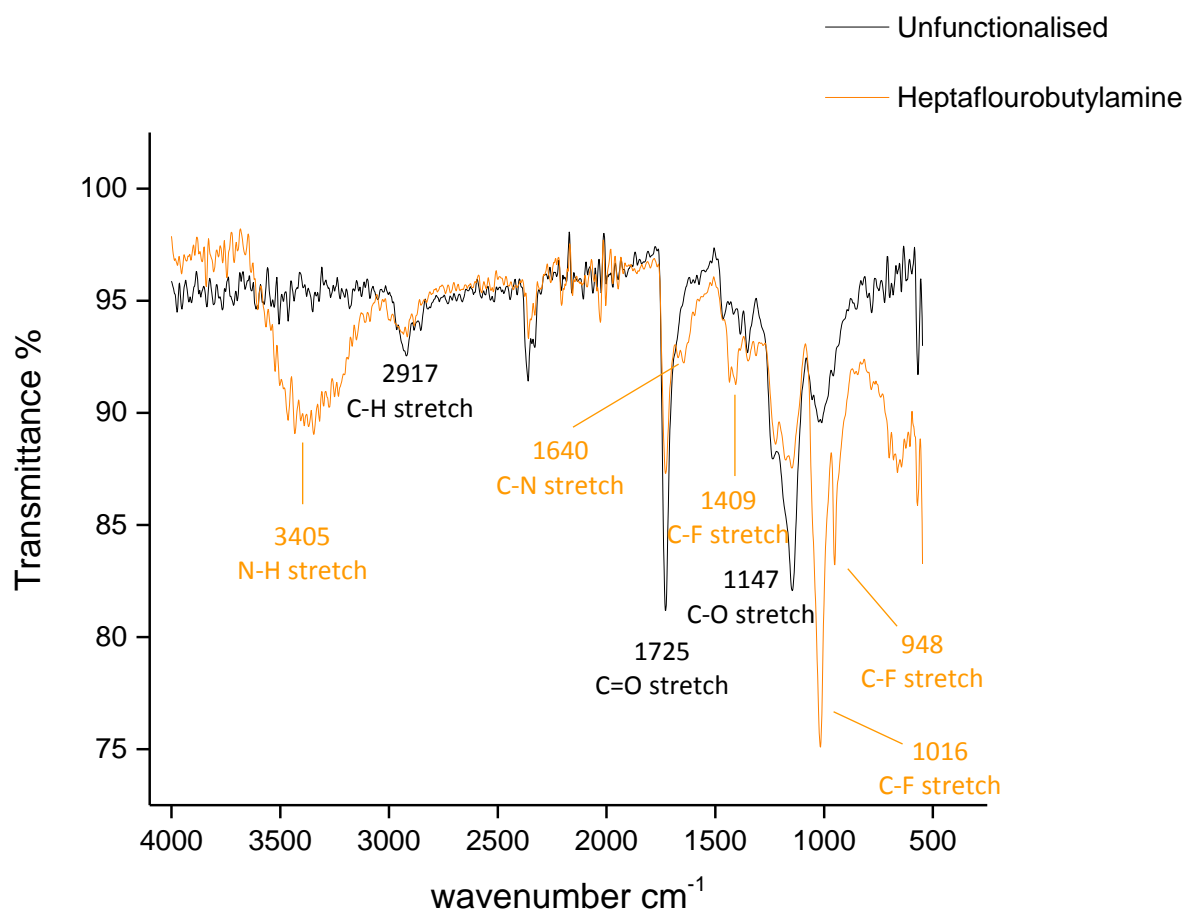


**Figure 5.** FT-IR spectra of unfunctionalized (black) and sulfo-SANPAH plus heptafluorobutylamine functionalized (orange) polyHIPE materials. All samples were thoroughly washed and dried prior to scanning.

Physically adsorbed proteins are susceptible to instability due to desorption over time as well as denaturation or misfolding on a given surface.<sup>[34,35]</sup> Fibronectin was both physically adsorbed onto polyHIPE scaffolds and attached covalently *via* sulfo-SANPAH. The extent of fibronectin functionalization was investigated by XPS (**Figure 6**).

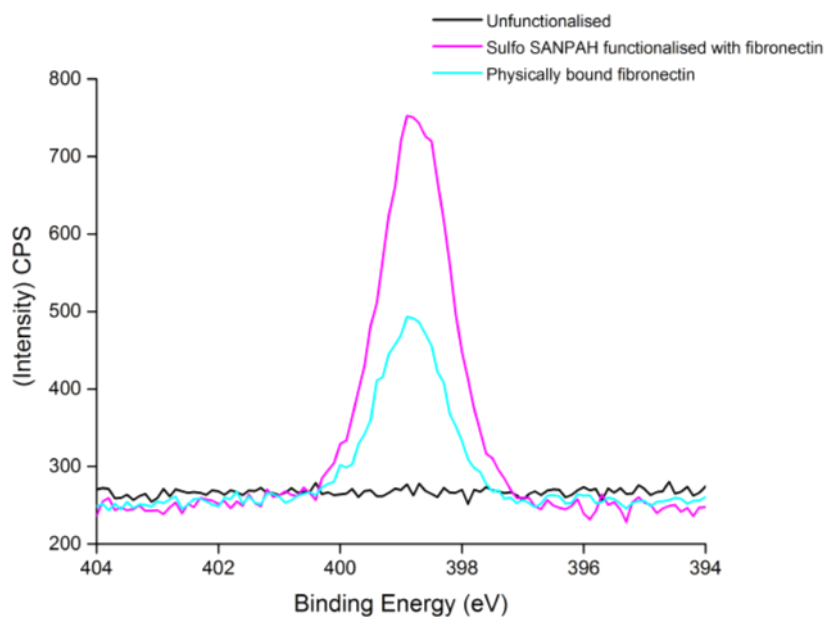


**Figure 6.** Overlaid high resolution N 1s spectra for unfunctionalized, sulfo-SANPAH functionalized with fibronectin and physically adsorbed fibronectin.

Sulfo- SANPAH functionalized with fibronectin displayed the highest N 1s concentrations, as expected due to covalent immobilisation of protein. Extensive washing of the physically adsorbed fibronectin caused the N 1s peak to diminish and the total C:N ratios from XPS were found to be 8.1:1 (before washing), and 21.1:1 (after washing).

Thiol-acrylate polyHIPEs are hydrophobic, however functionalization with hydrophilic molecules, such a bis-amino PEG and fibronectin, increases the hydrophilicity of the surface. The hydrophilicity of the PEG-bis-functionalized polyHIPE was examined by adding a 10  $\mu$ L drop of aqueous red food dye solution onto an unfunctionalized and a sulfo-SANPAH plus bis-amino PEG functionalized scaffold as shown in **Figure 7**.



**Figure 7.** Surface wettability of unfunctionalized (left) and sulfo-SANPAH plus bis-amino PEG functionalized scaffolds (right) at room temperature. Images were taken 30s after addition of the droplet.

The unfunctionalized scaffold was found to be relatively hydrophobic; the water droplet held its spherical shape, remained on the surface and was not absorbed into the polyHIPE through capillarity. The enhanced hydrophilicity of the PEG-bis functionalized scaffold allowed the droplet to spread extensively on the polyHIPE surface and most of its volume penetrated through the surface into the bulk. These results demonstrate that a hydrophilic, water absorbing, porous structure can be produced by surface functionalizing with hydrophilic molecules.

Primary human endometrial stromal cells (HESCs) were cultured on unfunctionalized and functionalized polyHIPE scaffolds to evaluate the influence of functionalization on cell adhesion, infiltration and function. HESCs were initially seeded onto unfunctionalized, physically adsorbed, sulfo-SANPAH and sulfo-SANPAH plus fibronectin scaffolds, cultured for up to 5 days and stained with haematoxylin/eosin (H & E). The cells adhered to the surface of the scaffolds, exhibiting a multilayer structure. Sulfo-SANPAH plus fibronectin functionalized scaffolds demonstrated the highest initial adhesion followed by unfunctionalized plus fibronectin scaffolds as shown in **Figure 8**.

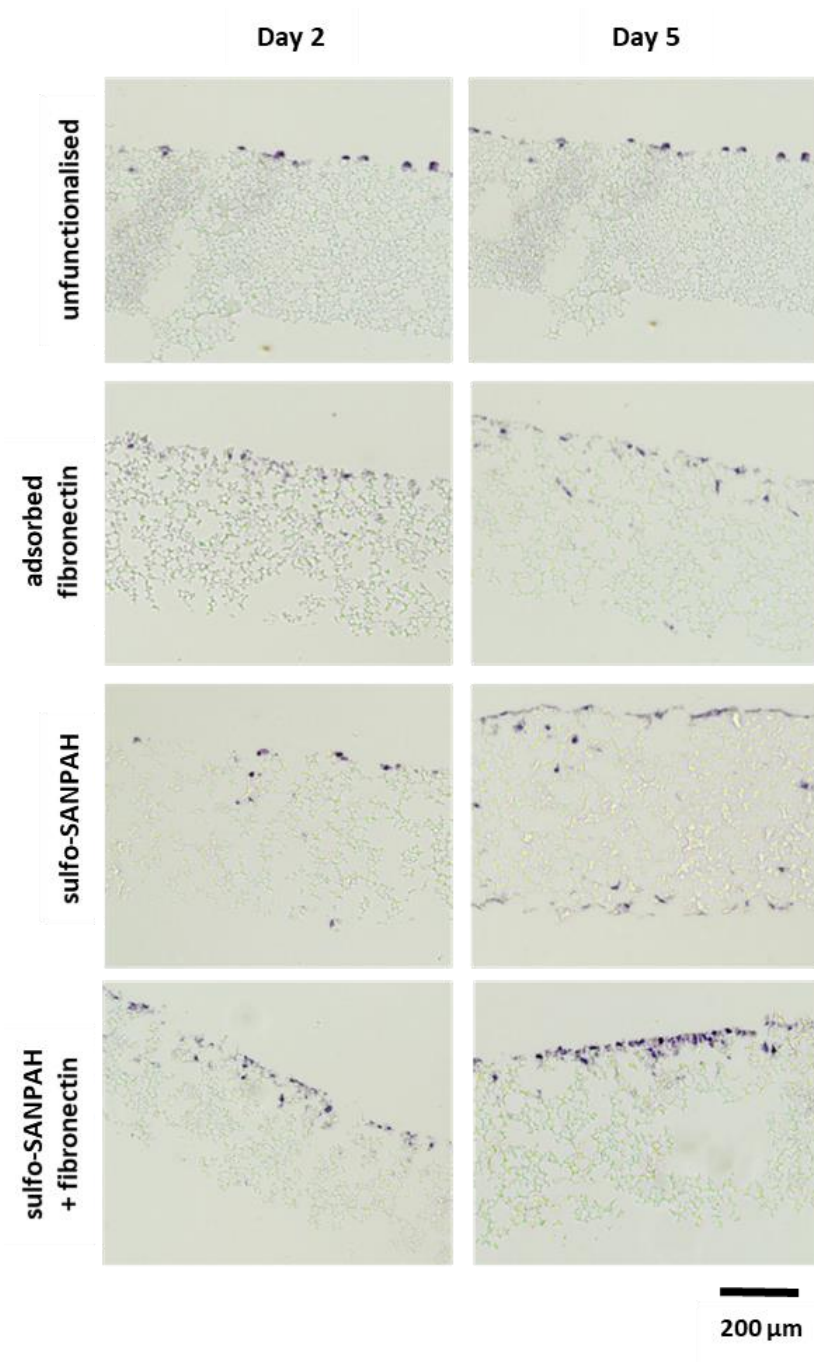


**Figure 8.** H & E stained sections of unfunctionalized, adsorbed fibronectin-, sulfo-SANPAH- and sulfo-SANPAH plus fibronectin-functionalized materials following culture of HESCs for 2 and 5 days. Scale bar = 200  $\mu$ m.

By day 5 of culture, significant cell infiltration in the sulfo-SANPAH plus fibronectin functionalized scaffolds was observed compared to the adsorbed fibronectin scaffold. Sulfo-SANPAH alone showed increased cell adhesion compared to the unfunctionalized scaffolds.

This suggests that sulfonate groups promote cell attachment as suggested by others<sup>[36,37]</sup> and is highlighted by an increased cell number on sulfo-SANPAH functionalized scaffolds. Cell number and viability were quantified by the LUNA™ automated cell counter. The total number of infiltrating cells at each time-point was determined by analysing three images of each scaffold stained with haematoxylin and eosin. The absolute cell count is depicted in **Figure 9** and a relative cell count presented in the ESI Figure SI-5. Over 5 days, on average, sulfo-SANPAH functionalized plus fibronectin scaffolds compared to adsorbed fibronectin scaffolds displayed a 122 % increase of cells on the scaffold surface. From the quantitative values and the histology images, the two optimal scaffolds were adsorbed fibronectin and sulfo-SANPAH-functionalized plus fibronectin. These scaffolds were then optimised further for cell function experiments.

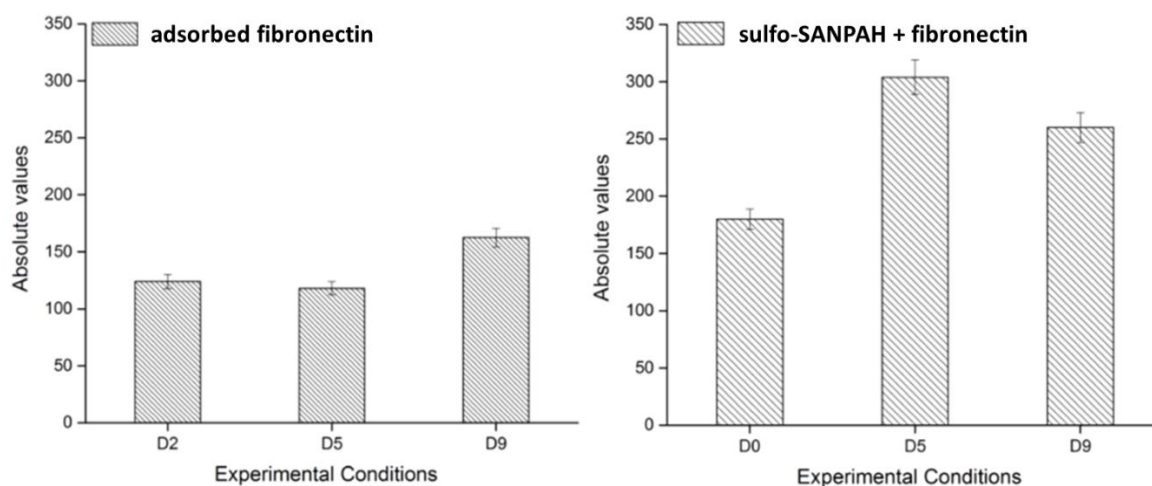


**Figure 9:** Absolute cell count for adsorbed fibronectin and sulfo-SANPAH-functionalized plus fibronectin scaffolds analysed from H & E stained images. Y axis maxima set to 350 to visualize comparisons.

Induction of *PRL* mRNA expression in response to 8-bromo-cAMP (cAMP, 0.5 mM) and medroxyprogesterone acetate (MPA,  $10^{-6}$ M) was evaluated as a marker of differentiation potential of HESCs. During the mid-luteal phase of the menstrual cycle, HESCs differentiate

into specialized decidual cells that control embryo implantation.<sup>[38]</sup> *PRL* transcript levels were quantified by real time quantitative polymerase chain reaction (RTqPCR) in three technical replicates (n=3) for each scaffold type. *PRL* mRNA levels, normalized to *LI9*, were expressed fold-change relative to expression levels in undifferentiated cells (D0) grown in the unfunctionalized scaffold.

As shown in Figure 10, expression of decidual *PRL* increases in response to cAMP and MPA signalling for 4 days (D4) in both the adsorbed fibronectin and fibronectin-functionalized scaffolds. Notably, basal *PRL* levels in undifferentiated cells (D0) and treated cells were higher in cells seeded on fibronectin-functionalized scaffolds, in line with the known role of fibronectin in providing an extracellular framework that stabilizes the decidual cytoskeleton and functional differentiation.<sup>[39,40]</sup>

Further work will look into optimizing the protocol of seeding more cells onto the scaffold, including the use of basic fibroblast growth factor (bFGF) and TGF $\beta$  inhibitors, which enhance proliferation by maintaining cells in a more naïve state.<sup>[41,42]</sup>

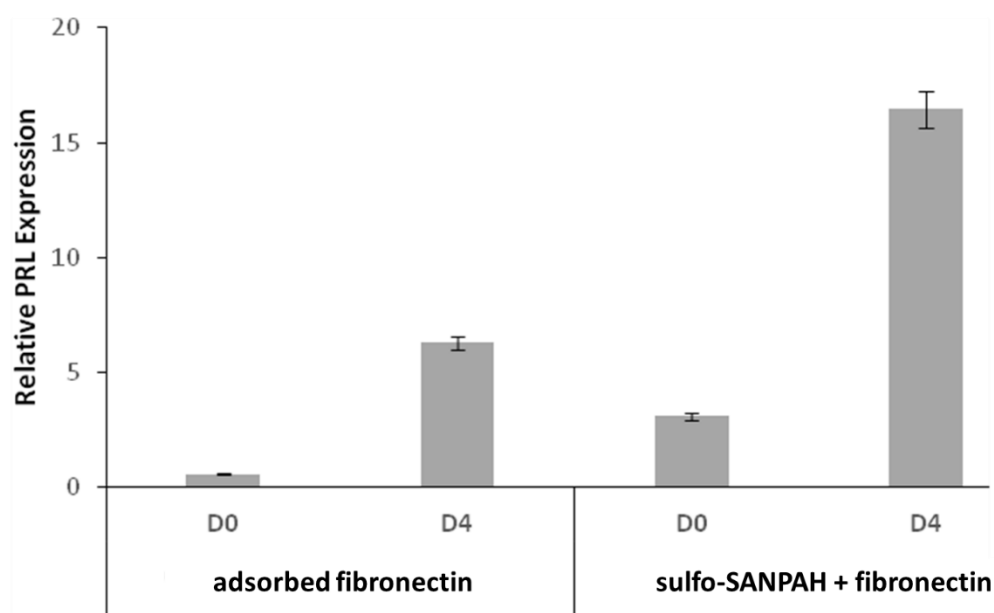


**Figure 10.** PRL activity after decidualization for 4 days. Data is normalized to D0 adsorbed fibronectin.

## **4. Conclusions**

In summary, we report a simple, versatile and efficient two-step conjugation method to covalently link selected compounds and biomolecules onto thiol-acrylate polyHIPE materials. Surface functionalization allows enhanced performance in cell interactions without sacrificing the physical properties of the polyHIPE, such as porosity and morphology. The sulfo-SANPAH reaction is a quick and convenient method carried out under high intensity UV light, allowing efficient attachment of sensitive biomolecules. XPS, fluorescence imaging and FTIR spectroscopy were used to investigate the functionality on the polyHIPEs surface and demonstrate successful conjugation. Importantly, the covalently-coated fibronectin polyHIPE materials promoted adhesion, infiltration and function of primary human endometrial stromal cells, highlighting polyHIPE scaffolds as a promising tool for endometrial research. We believe that the scope of this functionalization approach with sulfo-SANPAH has the potential to conjugate a wide range of molecules, such as proteins, enzymes and peptides to the surface of polyHIPE materials. Therefore, the approach described here may represent the next generation of polyHIPE scaffolds with tailored surface functionality, enhancing their application in 3D cell culture and tissue engineering whilst broadening the scope of applications to a wide range of cells.

## **Supporting Information**

Supporting Information is available from the Wiley Online Library or from the author.

## **Acknowledgements**

We would like to thank the Monash-Warwick Alliance for financial support. This work was funded in part by a National Institute for Health Research Blood and Transplant Research Unit

(NIHR BTRU) in red cell products in partnership with NHS Blood and Transplant. The views expressed are those of the author(s) and not necessarily those of the NHS, the NIHR or the Department of Health.

## Conflict of Interest

The authors declare no conflict of interest.

## Keywords

polyHIPEs; porous polymer scaffolds; surface functionalization; 3D cell culture; endometrial tissue.

Received: Month XX, XXXX; Revised: Month XX, XXXX; Published online:

((For PPP, use “Accepted: Month XX, XXXX” instead of “Published online”)); DOI: 10.1002/marc.((insert number)) ((or ppap., mabi., macp., mame., mren., mats.))

- [1] E. Y. Lee, W. H. Lee, C. S. Kaetzel, G. Parry, M. J. Bissell, *Proc. Natl. Acad. Sci. U. S. A.* **1985**, 82, 1419.
- [2] K. Shield, M. L. Ackland, N. Ahmed, G. E. Rice, *Gynecol. Oncol.* **2009**, 113, 143.
- [3] E. Carletti, A. Motta, C. Migliaresi, *Methods Mol Biol* **2011**, 695, 17.
- [4] A. S. Hayward, A. M. Eissa, D. J. Maltman, N. Sano, S. A. Przyborski, N. R. Cameron, *Biomacromolecules* **2013**, 14, 4271.
- [5] X. Liu, P. X. Ma, *Ann. Biomed. Eng.* **2004**, 32, 477.
- [6] J. K. Hong, S. V. Madihally, *Tissue Eng. Part B Rev.* **2011**, 17, 125.
- [7] M. G. Schwab, I. Senkovska, M. Rose, N. Klein, M. Koch, J. Pahnke, G. Jonschker, B. Schmitz, M. Hirscherd, S. Kaskel, *Soft Matter* **2009**, 5, 1055.
- [8] I. Pulko, J. Wall, P. Krajnc, N. R. Cameron, *Chem. – A Eur. J.* **2010**, 16, 2350.
- [9] S. J. Pierre, J. C. Thies, A. Duréault, N. R. Cameron, J. C. M. Hest, van, N. Carette, T. Michon, R. Weberskirch, *Adv. Mater.* **2006**, 18, 1822.

- [10] R. Owen, C. Sherborne, T. Paterson, N. H. Green, G. C. Reilly, F. Claeysens, *J. Mech. Behav. Biomed. Mater.* **2016**, *54*, 159.
- [11] S. Caldwell, D. W. Johnson, M. P. Didsbury, B. A. Murray, J. J. Wu, S. A. Przyborski, N. R. Cameron, *Soft Matter* **2012**, *8*, 10344.
- [12] C. Fischbach, R. Chen, T. Matsumoto, T. Schmelzle, J. S. Brugge, P. J. Polverini, D. J. Mooney, *Nat. Methods* **2007**, *4*, 855.
- [13] A. S. Hayward, N. Sano, S. A. Przyborski, N. R. Cameron, *Macromol. Rapid Commun.* **2013**, *34*, 1844.
- [14] N. R. Cameron, *Polymer* **2005**, *46*, 1439.
- [15] H. Deleuze, R. Faivre, V. Herroquez, *Chem. Commun.* **2002**, 2822-2823.
- [16] W. Busby, N. R. Cameron, C. A. B. Jahoda, *Polym. Int.* **2002**, *51*, 871.
- [17] L. Kircher, P. Theato, N. R. Cameron, *Polym. (United Kingdom)* **2013**, *54*, 1755.
- [18] C. Chen, A. M. Eissa, T. L. Schiller, N. R. Cameron, *Polymer* **2017**, *126*, 395-401.
- [19] A. Barbetta, N. R. Cameron, S. J. Cooper, *Chem. Commun.* **2000**, 221-222.
- [20] E. Lovelady, S. D. Kimmins, J. Wu, N. R. Cameron, *Polym. Chem.* **2011**, *2*, 559.
- [21] I. Pulko, P. Krajnc, *Macromol. Rapid Commun.* **2012**, *33*, 1731.
- [22] D. W. Johnson, C. Sherborne, M. P. Didsbury, C. Pateman, N. R. Cameron, F. Claeysens, *Adv. Mater.* **2013**, *25*, 3178.
- [23] C. R. Langford, D. W. Johnson, N. R. Cameron, *Polym. Chem.* **2014**, *5*, 6200.
- [24] S. Mezhoud, M. Paljevac, A. Koler, B. Le Droumaguet, D. Grande, P. Krajnc, *React. Funct. Polym.* **2018**, *132*, 51-59.
- [25] A. M. Eissa, P. Wilson, C. Chen, J. Collins, M. Walker, D. M. Haddleton, N. R. Cameron, *Chem. Commun.* **2017**, *53*, 9789.
- [26] C. B. Khatiwala, S. R. Peyton, A. J. Putnam, *Am. J. Physiol. Cell Physiol.* **2006**, *290*, C1640.
- [27] X. Liu, J. M. Holzwarth, P. X. Ma, *Macromol. Biosci.* **2012**, *12*, 911.
- [28] M. W. Hayman, K. H. Smith, N. R. Cameron, S. A. Przyborski, *Biochem. Biophys. Res. Commun.* **2004**, *314*, 483.
- [29] F. Barros, J. Brosens, P. Brighton, *BIO-PROTOCOL* **2016**, *6*, 2028.
- [30] A. Barbetta, N. R. Cameron, *Macromolecules* **2004**, *37*, 3202.
- [31] C. E. Hoyle, T. Y. Lee, T. Roper, *J. Polym. Sci. Part A Polym. Chem.* **2004**, *42*, 5301.
- [32] C. N. Salinas, K. S. Anseth, *J. Tissue Eng. Regen. Med.* **2008**, *2*, 296.
- [33] J. W. Lee, Y. J. Park, S. J. Lee, S. K. Lee, K. Y. Lee, *Biomaterials* **2010**, *31*, 5545.

- [34] D. Gidalevitz, Z. Huang, S. Rice, *Proc. Natl. Acad. Sci.* **1999**, *96*, 2608.
- [35] A. Schwarz, J. S. Rossier, E. Roulet, N. Mermoud, M. A. Roberts, H. H. Girault, *Langmuir* **1998**, *14*, 5526.
- [36] H. Zhang, P. J. Molino, G. G. Wallace, M. J. Higgins, *Sci. Rep.* **2015**, *5*, 13334.
- [37] J. F. Stefanick, J. D. Ashley, B. Bilgicer, *ACS Nano* **2013**, *7*, 8115.
- [38] B. Gellersen, J. J. Brosens, *Endocr. Rev.* **2014**, *35*, 851.
- [39] B. Babiarz, L. Romagnano, S. Afonso, G. Kurilla, *Dev. Dyn.* **1996**, *206*, 330.
- [40] J. C. Irwin, D. Kirk, R. J. King, M. M. Quigley, R. B. Gwatkin, *Fertil. Steril.* **1989**, *52*, 761.
- [41] S. Gurung, J. A. Werkmeister, C. E. Gargett, *Sci. Rep.* **2015**, *5*, 15042.
- [42] M. Yu, L. Wang, Y. Hu, Z. min Lian, J. lian Hua, *J. Integr. Agric.* **2013**, *12*, 1839.

**A new surface functionalization approach of polyHIPE materials with a range of amine-containing compounds including the cell adhesion-promoting ECM protein, fibronectin,** is reported. This approach, which uses a heterobifunctional linker to enable amine attachment, is facile, efficient, versatile and benign. The fibronectin-conjugated polyHIPE scaffolds show improved adhesion and function of primary human endometrial stromal cells, obtained with written informed consent from patient biopsies.

